

LM-00K048
October 27, 2000

Dynamics of Bubbles Rising in Finite and Infinite Media

C.C. Maneri, P.F. Vassallo

NOTICE

This report was prepared as an account of work sponsored by the United States Government. Neither the United States, nor the United States Department of Energy, nor any of their employees, nor any of their contractors, subcontractors, or their employees, makes any warranty, express or implied, or assumes any legal liability or responsibility for the accuracy, completeness or usefulness of any information, apparatus, product or process disclosed, or represents that its use would not infringe privately owned rights.

Dynamics of Bubbles
Rising in Finite and Infinite Media

by

Charles C. Maneri¹ and Peter F. Vassallo

For Publication in the American Institute of Chemical Engineers Journal

Key Words: bubble, velocity, data, model, planar

Lockheed Martin Corporation
P.O. Box 1072
Schenectady, New York

¹ Author to whom correspondence should be addressed.

Abstract

The dynamic behavior of single bubbles rising in quiescent liquid Suva (R134a) in a duct has been examined through the use of a high speed video system. Size, shape and velocity measurements obtained with the video system reveal a wide variety of characteristics for the bubbles as they rise in both finite and infinite media. This data, coupled with previously published data for other working fluids, has been used to assess and extend a rise velocity model given by Fan and Tsuchiya. As a result of this assessment, a new rise velocity model has been developed which maintains the physically consistent characteristics of the surface tension in the distorted bubbly regime. In addition, the model is unique in that it covers the entire range of bubble sizes contained in the spherical, distorted and planar slug regimes.

Dynamics of Bubbles

Rising in Finite and Infinite Media

1.0 Introduction

Dispersed two-phase flow is encountered in a wide variety of commercial systems, including chemical reactors, electronic devices and refrigeration devices. From a design standpoint, it is useful to have a predictive capability, or calculational procedure, which describes the flow in such systems. In order to obtain a calculational procedure, mechanistic models describing particular two-phase flow phenomena must first be developed.

An important parameter of two-phase flow is the interfacial shear or drag between the phases. Since there is a direct analytical relationship between the drag coefficient and the terminal or rise velocity of an individual bubble, the development of a drag coefficient model for bubbly flow should include, as a first step, the development of a rise velocity model for individual bubbles. Such a model has been developed by Fan and Tsuchiya (1990), for the viscous and distorted bubble regimes in infinite media for a range of fluid types.

The purpose of this investigation was to obtain rise velocity data for bubbles rising in finite and infinite media in order to assess the validity of the Fan-Tsuchiya model, in particular for low vis-

cosity fluids, and extend its applicability for finite media. In this context, previously published data by Haberman and Morton (1953) for various working fluids are used to make additional comparisons with the model.

2.0 Experimental Investigation

The fluid used in this investigation was Suva R-134a, one of the relatively new class of nonchlorinated refrigerant fluids which does not deplete the ozone layer. This fluid is widely used in heat exchangers, air conditioning and refrigeration systems and is recommended as a replacement for R-113 and R-114. Aside from its practical importance, R-134a is also of scientific interest because of its very low liquid-to-vapor density ratio and low surface tension (7.3 and 0.0021 N/m, respectively, at 2.4 MPa).

The experimental techniques used to generate isolated bubbles, the methods of data acquisition and reduction, and an analysis of the experimental results are given below.

2.1 Test Facility Procedure

2.1.1 Bubble Generation

The test was conducted in a vertical duct having a hydraulic diameter of 0.485 cm and an aspect ratio (spacing-to-width) of 0.044. These test section dimensions facilitate the use of thin, transparent heater films that enable visual observations and are consistent with the flow and control capa-

bilities of the test loop. A planar duct was chosen for the experiments rather than a circular tube because the planar duct minimized distortion effects when viewing the bubbles with a video camera. Bubbles were initially introduced into the Suva test section by injecting Suva vapor from an external tank (~0.5 liter volume) which was filled with liquid Suva and heated to produce vapor. A 0.37 mm ID tube channeled the Suva vapor into the test section to produce bubbles, the frequency of which was controlled by a needle valve. Measurements were taken with this method when the bubbles appeared to be sufficiently far apart; however, it was difficult to generate truly isolated bubbles with this technique. Furthermore, since some overpressure was required in the test section to eliminate the possibility of boiling, the bubbles experienced some degree of condensation as they rose.

To eliminate condensation effects, pressurized nitrogen gas was used in place of Suva in the external tank, with the same valve and tube arrangement used to control the bubble formation. Bubble frequencies of less than 1Hz were achieved, which was judged to be sufficient to prevent the wake interactions between bubbles from affecting the terminal velocity. The bubble size was controlled by raising the test section pressure; as the pressure increased, the bubble diameter decreased. This method produced bubbles having equivalent diameters less than 1mm. The equivalent diameter is defined as the diameter of an equivalent sphere whose volume is equal to the actual bubble volume.

In order to generate larger "planar" bubbles, including planar slugs, it was necessary to alter the valve and tube arrangement between the nitrogen tank and test section. A 1.59 mm ID tube was used and a mechanical toggle switch was installed. With this arrangement, individual large bubbles and slugs were generated by quickly opening and closing the toggle valve. The fluid was given suf-

ficient time (greater than 15 seconds) to stabilize between injection of the slugs. All the bubble rise data was taken in 24 °C liquid Suva.

2.1.2 Data Analysis

A high speed video system was used to measure the bubble shape and velocity. The high speed video was equipped with a long distance microscope lens to allow for high magnification. The magnification factor used for small bubbles (< 2mm diameter) varied between 33.5 and 37.5 for a 33 cm monitor screen. This factor was calculated by scanning the camera over a known distance and dividing the monitor scan distance by the known distance. The field of view for the smaller bubbles was about 0.635 cm by 0.84 cm, located between 7.6 cm and 25.4 cm above the bubble generator, depending on the bubble size. For the larger bubbles and slugs (generated with the toggle valve), the magnification was decreased to encompass the test section width. At this magnification, some distortion was observed near the edges of the view. To improve accuracy, the magnification factor in the center of the view (where the bubbles were rising) was determined by measuring the width of a known reference dimension on the test section window as viewed on the monitor and dividing it by the known distance. The magnification factor for slugs was calculated to be about 3.8.

A strobe light was placed across from the video camera on the opposite side of the test section. It was used in concert with the video camera to track the bubbles within 0.004 second time steps. As the strobe light passed through the test section, it diffracted at the bubble surface, and produced a

dark diffraction ring around the bubble perimeter on the video image. Measurements of bubble size and velocity were obtained directly from the video image. An aspect ratio, E , was assigned to each bubble or slug, defined as the ratio of the vertical to horizontal dimension. The equivalent diameter, d_e , was determined based on calculations of the bubble or slug volume which was calculated using shapes that best approximated each bubble or slug: spheres and oblate spheroids for bubbles < 2.0 mm; planar ellipses for bubbles between 3.0 and 5.0 mm; planar circular segments for bubbles between 5.0 and 10.0 mm; and partial planar ellipses for slugs. The uncertainty of the measurements were as follows: ± 0.045 mm for diameter at high magnification; ± 0.4 mm for diameter at low magnification; $\pm 5\%$ for velocity at high magnification; and $\pm 2.2\%$ for velocity at low magnification. In addition, the uncertainty of calculating the equivalent bubble diameter from the video measurements is estimated to be: $\pm 2.2\%$ for $d_e < 2$ mm; 5-10% overestimate for $3 < d_e < 5$ mm; 2% overestimate for $5 < d_e < 10$ mm; $\pm 10\%$ for $d_e > 10$ mm.

2.2 Discussion of Experimental Results

The experimental results, including bubble equivalent diameter, bubble aspect ratio E and rise velocity, are presented in Table 1 and Figure 1. Distinct regions are observed based on the bubble shape and rise behavior. These regions are defined with respect to equivalent diameter, d_e . A brief description of each of these regions is given below. Some examples of the different classifications of bubbles and slugs are given in Figure 2.

Spherical

$0 < d_e < 0.25$ mm

For these bubbles, viscous forces dominate and their shape is closely approximated by a sphere. The rise velocity qualitatively obeys Stokes' law, which says that the bubble velocity is nearly proportional to the square of the diameter. The flow around these bubbles is smooth, with no separation occurring.

Ellipsoidal (Oblate Spheroidal)

$$0.25 < d_e < 1.0 \text{ mm}$$

As the bubble volume increases, the pressure force on the front surface of the bubble increases, and the bubbles flatten in the direction of motion. In this range, these bubbles are oblate with a convex interface (viewed from inside) around the entire surface. The rise velocity increases with bubble diameter up to a peak velocity of about 20 cm/s. At this point, the bubble becomes too large for the fluid streamlines to smoothly reattach behind the bubble and a turbulent wake is formed. This wake, called a toroidal vortex, grows as the bubble diameter increases and, as a result, the rise velocity gradually decreases. The vortex wake for these ellipsoidal bubbles reattach downstream of the bubbles in a relatively steady manner.

Ellipsoidal (Oblate Spheroidal) - Oscillatory

$$1.0 < d_e < 2.5 \text{ mm}$$

When the bubble diameter approaches 1.0 mm, the vortex wake no longer reattaches in a steady manner, and axisymmetric vortex sheets roll inward to produce oscillations. The bubbles oscillate in shape as they rise, first narrowing in the width direction while expanding in the height direction, then vice versa. The aspect ratio in Figure 1 for these bubbles (taken as the minimum observed aspect ratio) is somewhat higher than that of ellipsoidal bubbles of smaller diameter.

This behavior appears to be associated with variations in the wake structure as the bubble volume-rise velocity relationship changes with increasing bubble volume. These variations alter the pressure acting on the underside of the bubble which can either compress or elongate the bubble in the vertical direction.

Ellipsoidal - Wobbly

$$2.5 < d_e < 5.0 \text{ mm}$$

These bubbles are large enough to fill the duct spacing, with a liquid film present between the sides of the bubbles and the walls. The film is rippled due to perturbations from the bubble. In this range of bubble sizes, vortex shedding from the bubble wake is initiated which causes the bubbles to wobble, stretch and distort about a planar elliptical shape as they rise. The rise velocity, having reached a minimum in the oscillatory region, again begins to increase with increasing equivalent diameter. This is because the buoyancy force begins to dominate the flow.

Cylindrical (Planar) Cap

$$5.0 < d_e < 10.0$$

Bubbles in this region resemble segments cut from a planar circle, with a flat bottom and a circular top or "cap". The liquid film between the bubble and the duct wall in the spacing direction is very thin, with little or no ripples present. The frontal surface of the bubble is usually stable, while the rear surface may wobble, deform and/or rock because of asymmetric vortex shedding. The aspect ratio of these bubbles is relatively uniform, with measured values of about 0.31.

Slug

$$d_e > 10.0 \text{ mm}$$

In this region the rise velocity reaches a constant value of approximately 18.0 - 19.0 cm/sec regardless of bubble volume. Bubbles in this region are termed slugs, although in the early stages of this region the bubbles are still cylindrical caps. In fact, the slug limit, or incipient slug size, (based on the rise velocity value) is reached when the width of the base of the bubbles is approximately two-thirds of the test section width. As the bubble size is increased beyond 10.0 mm, the bubble shape transitions to the shape of a classical planar slug (see Figure 2) which is characterized by an unchanging frontal shape as the bubble volume is increased. Since the bubble is now constrained in the widthwise direction, the axial length of the bubble increases more rapidly than the width as the bubble size is increased; consequently, the aspect ratio increases monotonically from the constant cylindrical cap value of 0.31 as seen in Figure 1.

A comparison of these bubble shape types/regimes with those reported by Grace, *et al.* (1973) for bubbles rising in infinite media is given in Figure 3 as a function of the dimensionless Eotvos, Morton and Reynolds numbers, which are defined as

$$Eo = \frac{\Delta\rho g d_e^2}{\sigma} \quad (1)$$

$$Mo = \frac{g \mu_l^4 \Delta\rho}{\rho_l^2 \sigma^3} \quad (2)$$

$$Re = \frac{\rho_l U d_e}{\mu_l} \quad (3)$$

The comparison shows that the bubble types/regimes observed in this investigation are consistent

with the results of other investigators.

3.0 Analytical Investigation

In this section, the Fan-Tsuchiya rise velocity model is described and evaluated relative to the experimental Suva results.

The Fan-Tsuchiya model for single bubbles rising in infinite media is given by

$$U_{\infty} = [U_V^{-\eta} + U_D^{-\eta}]^{-1/\eta} \quad (4)$$

where U_V is the rise velocity in the viscous regime (see Figure 1) which has the form:

$$U_V = \frac{g\Delta\rho d_e^2}{K_b\mu_l} \quad (5)$$

and U_D is the rise velocity in the distorted-inertial regime which has the form given by Mendelson (1967):

$$U_D = \left[g \frac{d_e \Delta\rho}{2 \rho_l} + \frac{2c\sigma}{\rho_l d_e} \right]^{1/2} \quad (6)$$

Here c is a multiplier on the static surface tension σ , ranging from 1.0 to 2.0 depending upon the

fluid, and K_b is a parameter given by

$$K_b = \max \text{ of } \begin{cases} 12.0 \\ K_{bo} Mo^{-0.038} \end{cases} \quad (7)$$

where $K_{bo} = 10.2$ for organic solvents and mixtures, and 14.7 for aqueous solutions. It should be noted that the parameter c was introduced into the Mendelson relation (Eq. (6)) by Fan and Tsuchiya to extend its applicability to pure, or clean, multicomponent fluids since, as noted by Mendelson, Eq. (6) underestimates the terminal velocities in multicomponent fluids when $c = 1.0$. Physically, the introduction of c can be rationalized by the concept of a dynamic surface tension which tends to be greater than the static value for pure multicomponent fluids. Evidence of large differences in the measured surface tension of dynamic vs. static interfaces has been reported by Jontz and Meyers (1960).

For a finite medium, Eq (4) must be modified to account for wall effects. Based on the work of Maneri (1995), the rise velocity in a noncircular duct of width W is given by

$$U = U_{\infty} \left[\tanh \frac{c_1 W}{d_e} \right]^{1/2} \quad (8)$$

where U_{∞} is given by Eq (4) and c_1 is obtained from the relationship

$$c_1 = \beta \tanh^{-1} \left[\frac{U_s}{U_{\infty}(d_e = \beta W)} \right]^2 \quad (9)$$

The parameter β is the ratio of the equivalent diameter to the duct width for a cylindrical cap bubble whose maximum dimension in the width direction is equal to two-thirds of the channel width. As previously mentioned, this is the minimum bubble size, or incipient slug size, at which the slug terminal velocity limit U_s is reached. An expression for the slug limit is given by

$$U_s = 0.2445[1 + 0.82(t/W) - 0.368(t/W)^2] \left[gW \frac{\Delta\rho}{\rho_l} \right]^{1/2} \quad (10)$$

which was obtained from a fit of the data of Griffith (1963) and Maneri (1974).

3.1 Comparison with Experimental Results

The Suva rise velocity data obtained in this investigation are compared with the Fan-Tsuchiya model in Figure 4 using the values of $c = 1.2$ and $\eta = 1.6$ as recommended by Fan-Tsuchiya. It is evident that the model does not completely predict the Suva data over the entire range of bubble sizes. This is especially true in the viscous regime where the experimental values are significantly underpredicted. In view of this, it was decided to take a closer look at the Fan-Tsuchiya rise velocity model.

3.2 Review of Fan-Tsuchiya Model

First, a comparison of the Fan-Tsuchiya model in the viscous regime (Eq. (5)) with water and turpentine data obtained by Haberman and Morton (1953) and Freon data obtained by Vassallo, *et al.* (1995) is given in Figure 5 on a log-log basis. It is seen that, in all cases, the equivalent diameter

exponent of 2.0 (slope of 2.0 in Figure 5) does not accurately predict the trend in the data.

Second, in the distorted-inertial regime, Fan and Tsuchiya, in an apparent inconsistency, recommend a value of $c = 1.2$ in Eq (6) for clean monocomponent fluids, inferring that the surface tension for these fluids is greater under dynamic conditions than under static conditions. There is no physical basis for this inference, however. In fact, the data for the two clean monocomponent fluids used by Fan and Tsuchiya to develop their model - distilled water and methonal - are well predicted by Eq (6) with $c = 1.0$, as shown in Figure 6.

As a result of these observations, a new model was developed as described in the following section.

4.0 Development of the Rise Velocity Model

The rise velocity model was developed under the following constraints:

- the basic structure of the Fan-Tsuchiya model as extended for finite media be preserved
- the Mendelson equation (Eq (6)) remain unaltered (i.e., $c = 1.0$) for clean monocomponent fluids
- the basic form of the rise velocity expression for the viscous regime (Eq (5)) be maintained

In order to satisfy the third constraint in view of the first observation of Section 3.2, the dimensionless parameter K_b was taken to be a function of the equivalent diameter as well as the Morton number, or

$$K_b = f(Mo)d_e^a \quad (11)$$

In this form, $f(Mo)$ is a dimensional quantity. A more desirable form is obtained by dividing d_e by a characteristic length d_o , so that K_b can be expressed as

$$K_b = f(Mo)\left(\frac{d_e}{d_o}\right)^a \quad (12)$$

where d_o is chosen to be

$$d_o = 2.0\left[\frac{\sigma}{\Delta\rho g}\right]^{1/2} \quad (13)$$

which is the diameter corresponding to the minimum rise velocity given by the Mendelson equation.

With these modifications and constraints, a best overall fit of the available rise data was obtained with $a = 0.425$, $\eta = 8.0$, $c = 1.0$ and 1.4 for low viscosity mono and multicomponent fluids respectively, and the following functional form for $f(Mo)$:

$$f(Mo) = K(1.0 - e^{-5.31 \times 10^{10} Mo}) \quad (14)$$

where

$$K = \begin{cases} 148 \text{ aqueous solutions} \\ 60 \text{ organics} \end{cases} \quad (15)$$

A comparison of the model is given with monocomponent (water, methanol and Suva) and multi-component (turpentine and varsol) rise velocity data in Figures 7 through 11. Also included in the figures for comparative purposes is the original Fan-Tsuchiya model with its corresponding values for c and η . It is seen from the comparisons that, relative to the original Fan-Tsuchiya model, the new model provides a better overall prediction of the data while maintaining $c = 1.0$ for monocomponent fluids. Thus, the new model is not only more accurate, it is also more consistent with the physical characteristic of surface tension in the distorted bubbly regime.

Conclusions

It is shown that the wave analogy bubble rise model, originally proposed by Mendelson (1967) for bubbles rising in infinite media and extended by Maneri (1995) to bubbles rising in ducts of low aspect ratio, can be integrated with a modified Stokes flow model to obtain a single expression which describes the terminal velocity of single bubbles rising in mono and multicomponent fluids. The new model is applicable to bubble sizes and geometries ranging from small spherical bubbles to large planar slugs. The model predictions compare well to previously published data as well as to the Suva data obtained in this investigation over the entire bubble size range. Based on these comparisons, it is concluded that the new model may be used as a general predictive tool for bubble rise velocity in finite and infinite media.

Notation

g = gravitational constant

U = rise velocity

W = duct width

t = duct spacing

Greek Symbols

ρ = fluid density

$\Delta\rho$ = density difference between liquid and gas

σ = surface tension

μ = dynamic viscosity

η = exponent in Fan-Tsuchiya equation

Subscripts

g = gas

l = liquid

Literature Cited

Fan, L.S. and Tsuchiya, K., *Bubble Wake Dynamics in Liquids and Liquid-Solid Suspensions*, Butterworth-Heinemann, Stoneham, MA (1990).

Grace, J.R., Wairegi, T., and Nguyen, T.H. "Shapes and Velocities of Single Drops and Bubbles Moving Freely Through Immiscible Liquids," *Trans. Instn. Chem. Engrs.*, **54** (1973).

Griffith, P., "The Prediction of Low Quality Boiling Voids," ASME Paper 63-HT-20 (1963).

Haberman, W.L. and Morton, R.K., "An Experimental Investigation of the Drag and Shape of Air Bubbles Rising in Various Liquids," David Taylor Model Basin, Report 802 (1953).

Jontz, P.D. and Meyers, J.E., "The Effect of Dynamic Surface Tension on Nucleate Boiling Coefficients," *AIChE J.*, **6**, 34 (1960).

Maneri, C.C. and Zuber, N., "An Experimental Study of Plane Bubbles Rising at Inclination," *Int. J. Multiphase Flow*, **1**, 623 (1974).

Maneri, C.C., "New Look at Wave Analogy for Prediction of Bubble Terminal Velocities," *AIChE J.*, **41** (1995).

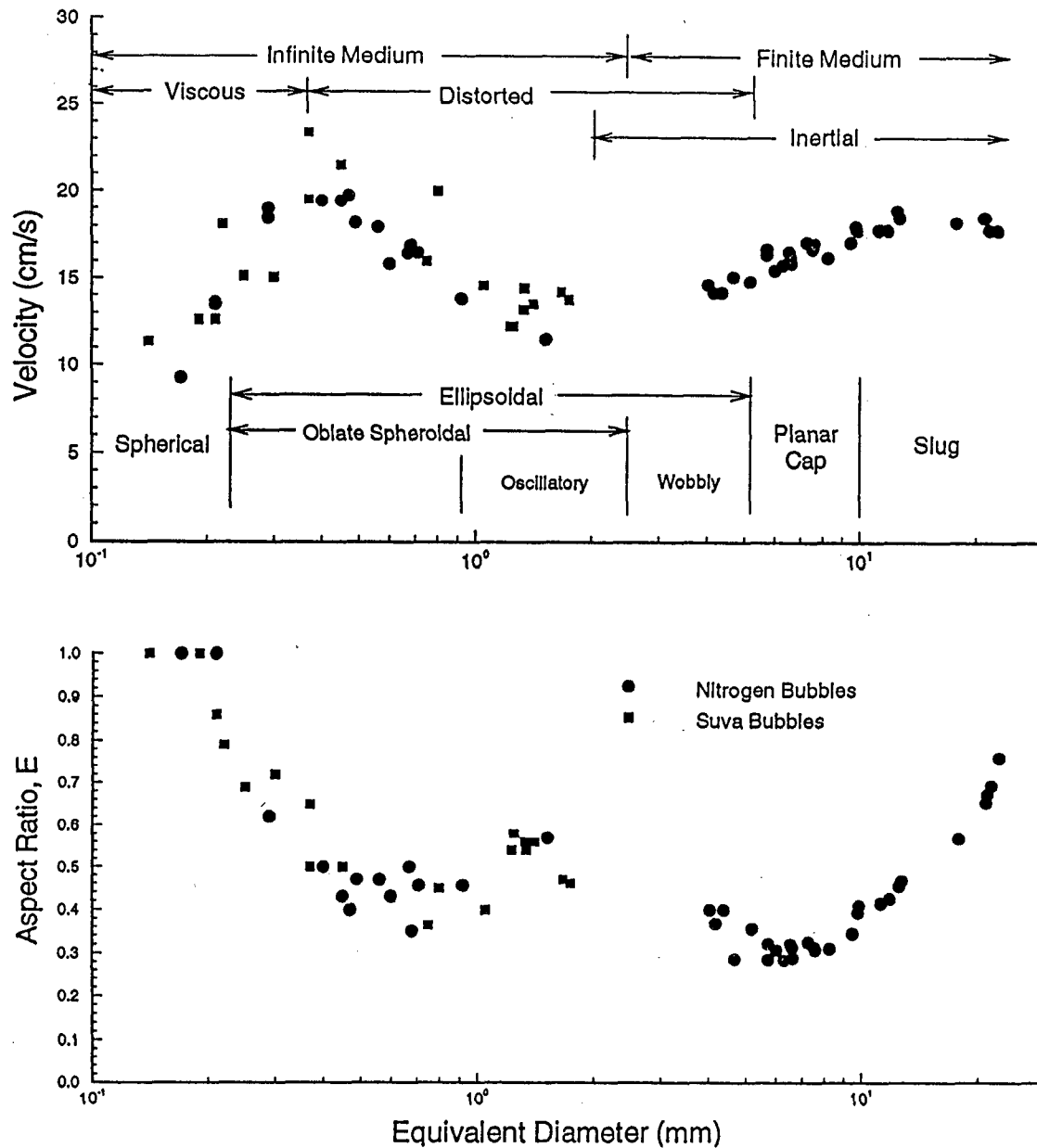
Mendelson, H.D., "The Prediction of Bubble Terminal Velocities from Wave Theory," *AIChE J.*, **13**, 250 (1967).

Vassallo, P.F., Symolon, P.D., Moore, W.E., and Trabold, T.A., "Freon Bubble Rise Measurements in a Vertical Rectangular Duct," *J. Fluids Engr.*, **117**, (1995).

Table 1
Bubble Rise Data in Liquid Suva






Nitrogen Bubbles			Suva Bubbles		
<u>de(mm)</u>	<u>U(cm/s)</u>	<u>E</u>	<u>de(mm)</u>	<u>U(cm/s)</u>	<u>E</u>
7.25	17.1	.325	.75	16.0	.364
5.71	16.4	.285	1.23	12.25	.54
6.0	15.5	.306	.45	21.5	.50
9.77	18.0	.394	1.25	12.25	.58
5.71	16.7	.321	.37	19.5	.65
21.2	18.5	.674	.19	12.62	1.0
12.73	18.5	.467	1.41	13.53	.56
6.61	15.9	.288	.22	18.1	.79
4.68	15.1	.286	1.05	14.56	.40
1.52	11.5	.570	.21	12.62	.86
9.46	17.11	.345	.14	11.36	1.0
21.0	18.5	.654	.30	15.07	.72
12.54	18.9	.455	.80	20.0	.45
6.58	16.2	.313	1.33	13.2	.56
4.17	14.2	.368	.37	23.4	.5
21.7	17.8	.694	1.67	14.2	.47
11.23	17.8	.416	1.34	14.42	.54
6.29	15.8	.284	.25	15.15	.69
7.51	16.74	.313	1.75	13.77	.46
17.85	18.24	.568			
8.24	16.22	.310			
11.84	17.78	.426			
22.8	17.78	.76			
9.83	17.78	.41			
4.03	14.63	.40			
7.57	17.0	.308			
5.18	14.84	.356			
4.37	14.2	.40			
6.52	16.54	.32			
0.92	13.82	.456			
0.71	16.47	.456			
0.67	16.47	.50			
0.68	16.9	.35			
0.60	15.84	.43			
0.56	17.95	.47			
0.47	19.71	.40			
0.29	18.48	.62			
0.49	18.19	.47			
0.21	13.5	1.0			
0.29	19.0	.62			
0.40	19.43	.50			
0.45	19.43	.43			
0.21	13.6	1.0			
0.17	9.3	1.0			


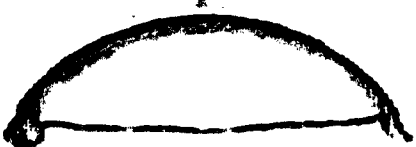
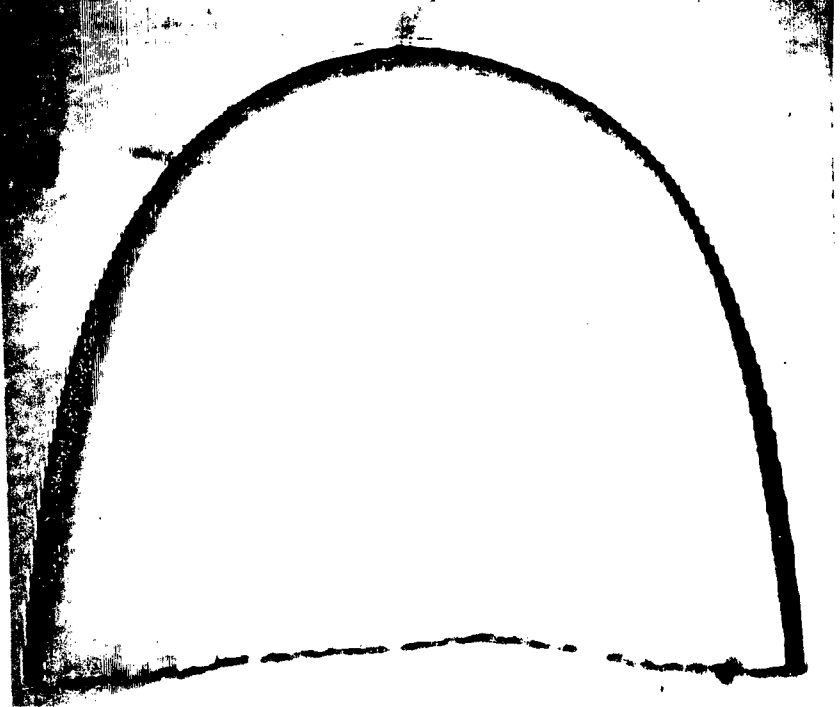
Figure 1
Terminal Velocity and Shape Data for
Nitrogen and Suva Bubbles Rising in Liquid Suva



20

Figure 2
Bubble Rise Video Images in Quiescent Liquid Suva ($T=24^{\circ}\text{C}$)

					
$d_e(\text{mm}) =$	0.17	0.29	0.47	0.68	1.34
$E =$	1.0	0.62	0.40	0.35	0.54
$V (\text{cm/s}) =$	9.3	18.5	19.7	16.9	14.4
Type =	Spherical	Elliptical	Elliptical	Elliptical	Oscillatory Ellipse

			
$d_e(\text{mm}) =$	4.9	7.7	22.8
$E =$	0.29	0.31	0.76
$V (\text{cm/s}) =$	15.1	16.7	17.8
Type =	Wobbly Ellipse	Planar Cap	Slug

18

Figure 3

Shape Regimes for Bubbles/Drops in Infinite Media

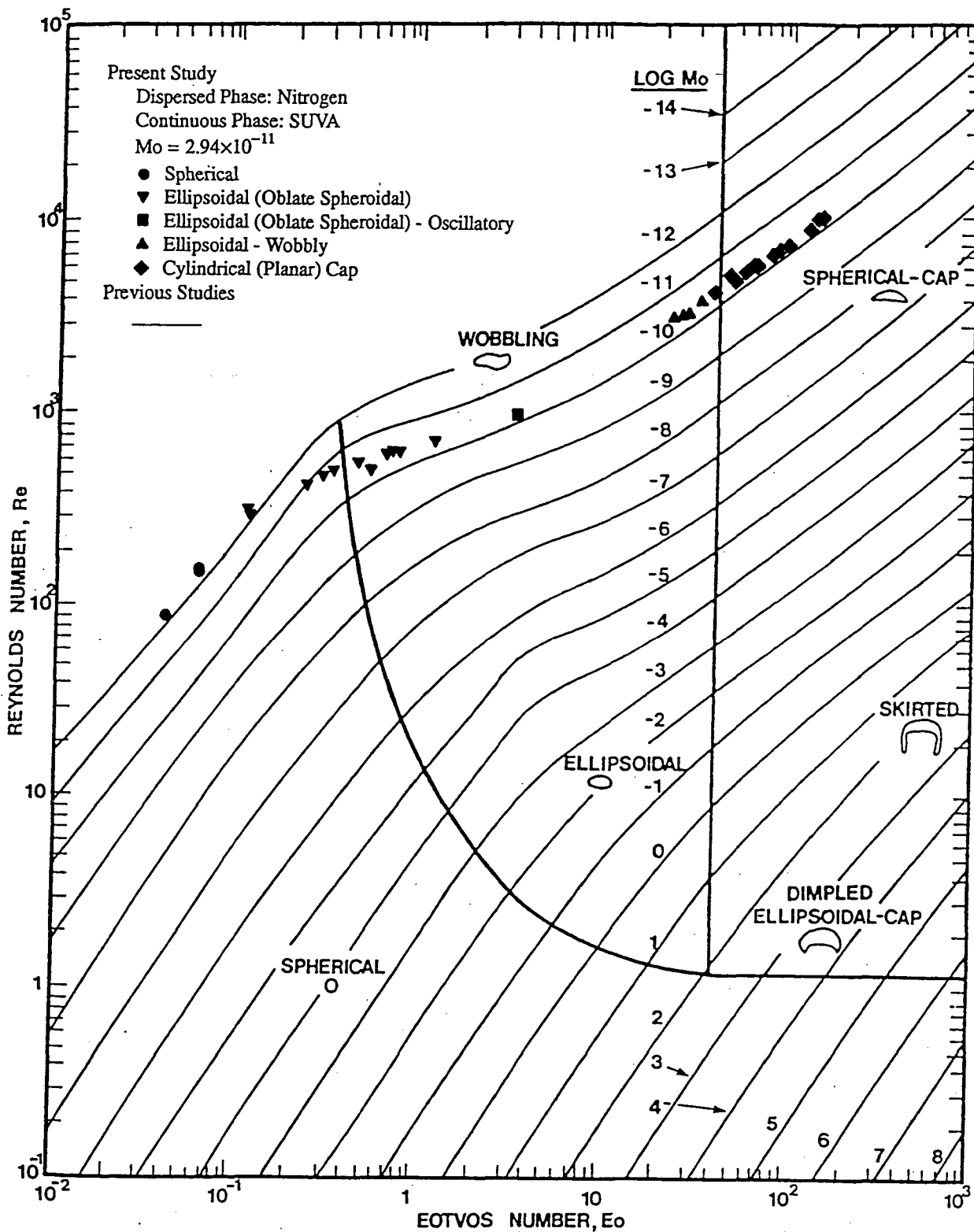
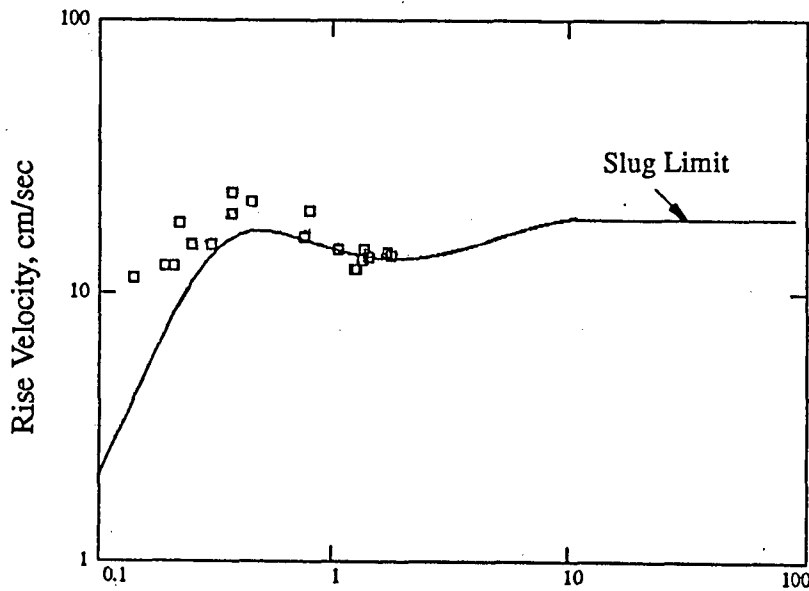
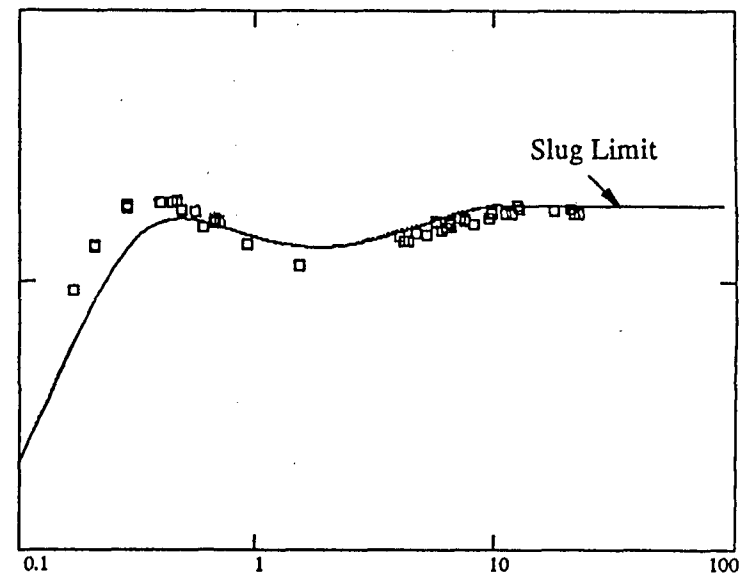


Figure 4
Comparison of Fan-Tsuchiya Model with Experimental SUVA Results

— $C=1.2$, $\eta=1.6$



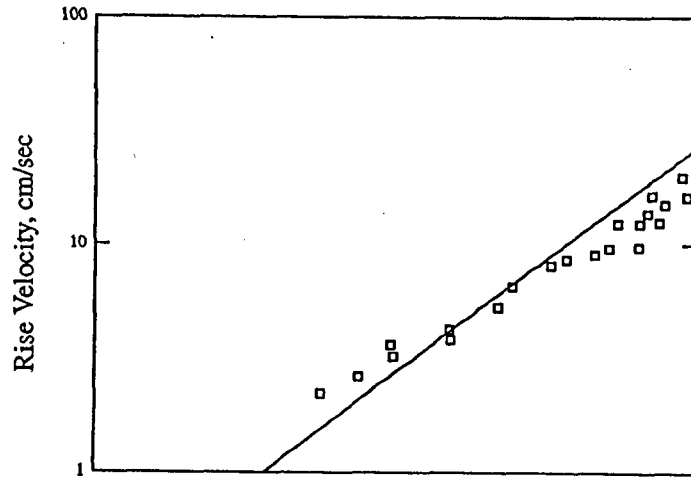
Equivalent Bubble Diameter, mm
(a) Dispersed Phase: SUVA



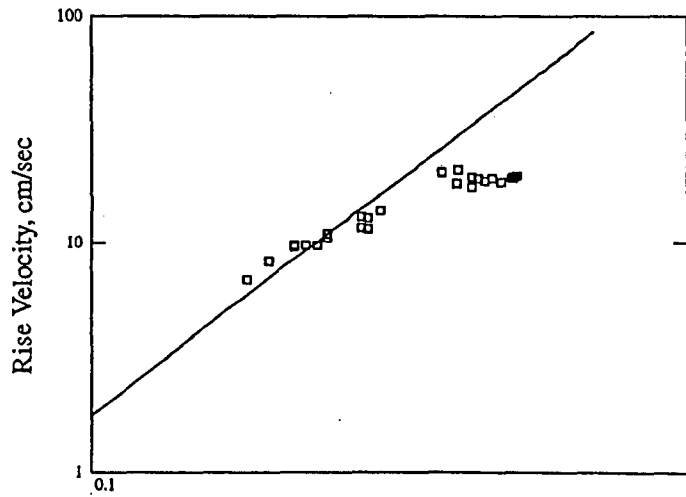
Equivalent Bubble Diameter, mm
(b) Dispersed Phase: Nitrogen

Figure 5

Comparison of Fan-Tsuchiya Model with Experimental Results - Viscous Regime

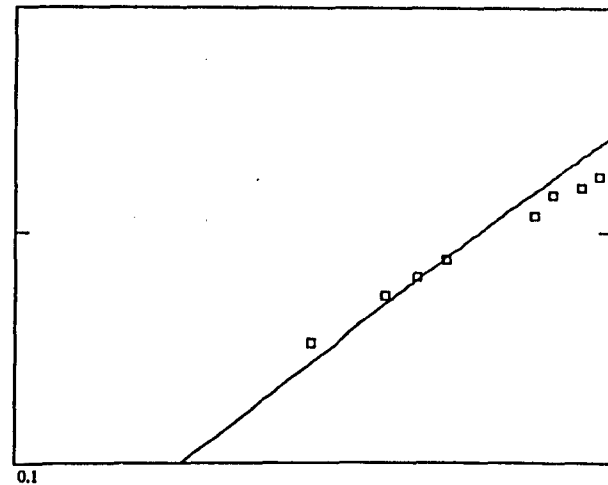


(a) Water



Equivalent Bubble Diameter, mm

(b) Freon



Equivalent Bubble Diameter, mm

(c) Turpentine

Infinite Medium

Dispersed Phase: Air

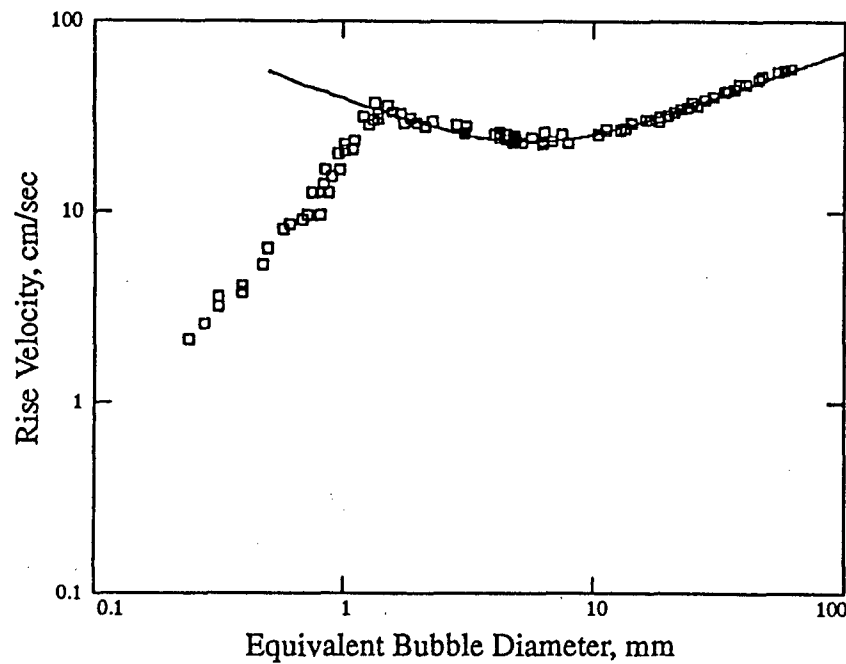
— Equations (5) and (7)

12

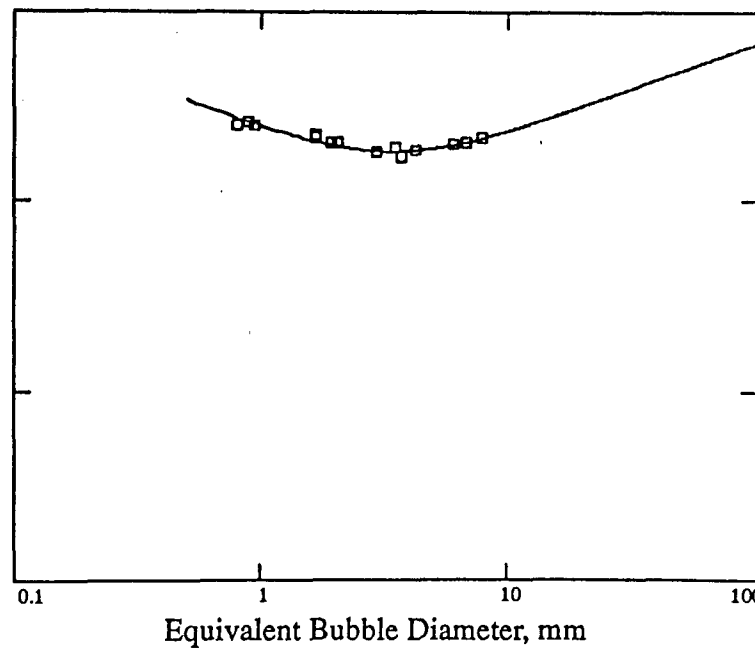
Figure 6
Comparison of Mendelson Model with Experimental Results - Distorted/Inertial Regime

Infinite Medium

— C=1.0



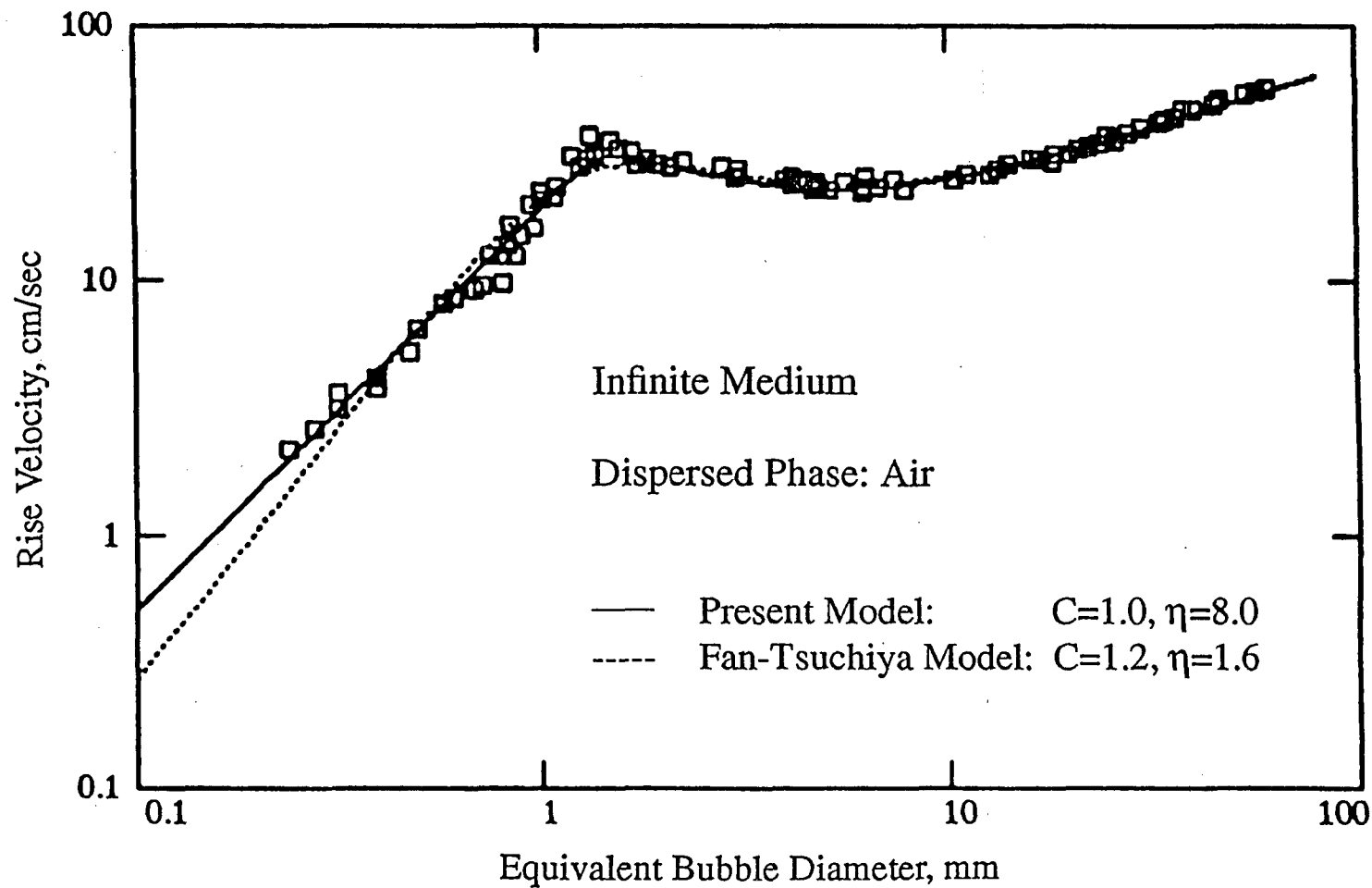
(a) Dispersed Phase: Air
Continuous Phase: Water



(b) Dispersed Phase: Air
Continuous Phase: Methanol

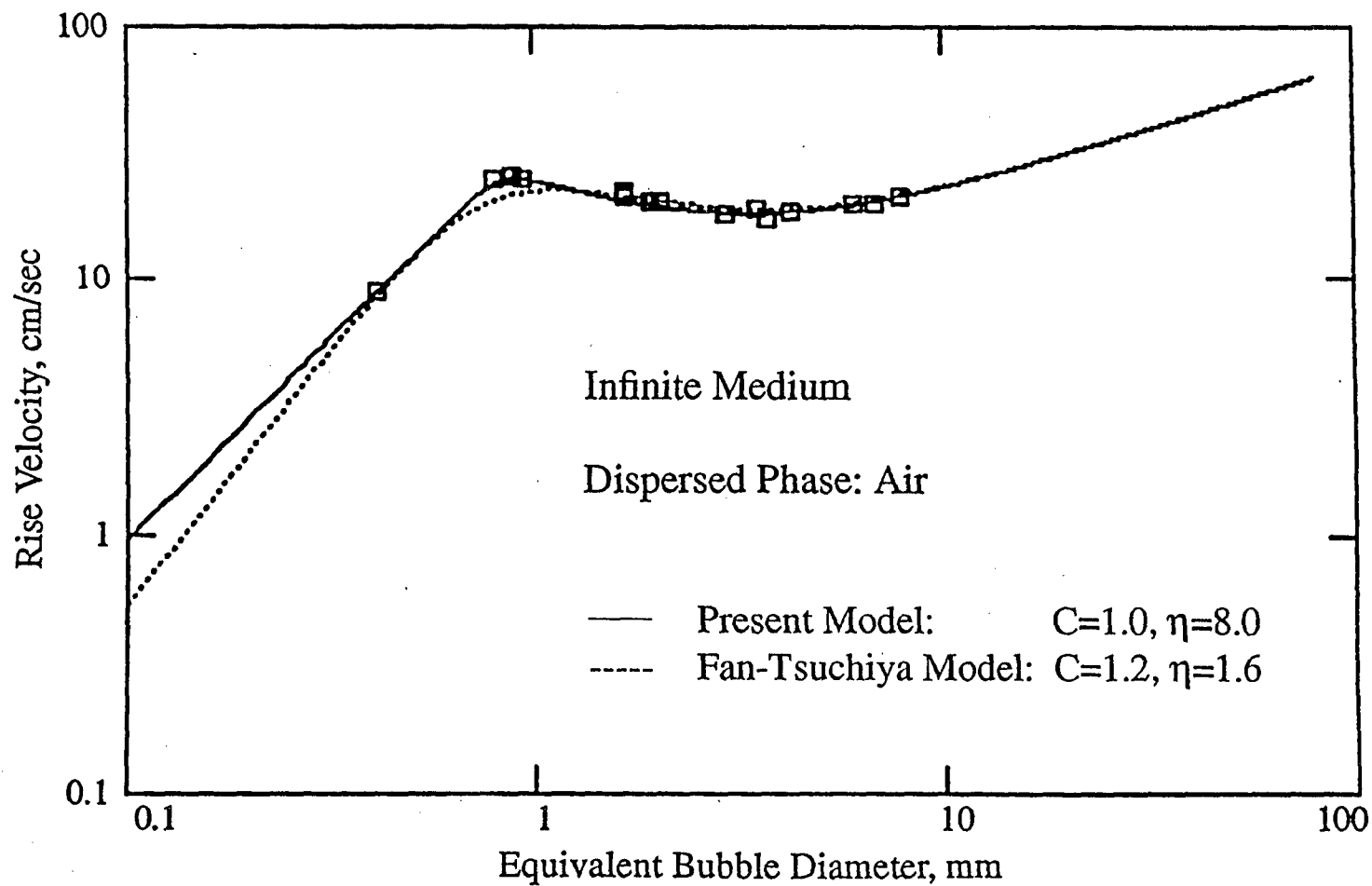
25

Figure 7
Comparison of Predicted Rise Velocity with
Experimental Water Results [Haberman and Morton, 1953]



92

Figure 8
 Comparison of Predicted Rise Velocity with
 Experimental Methanol Results [Haberman and Morton, 1953]

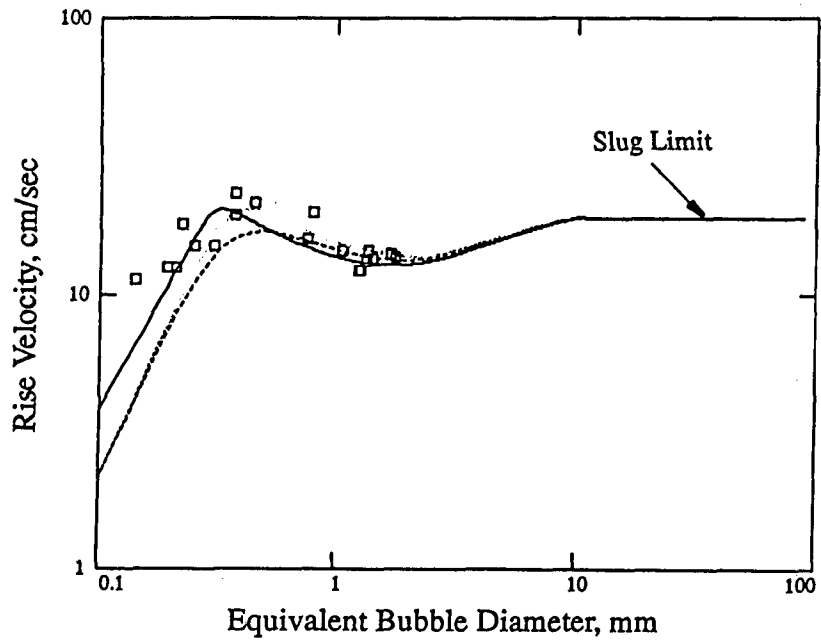


28

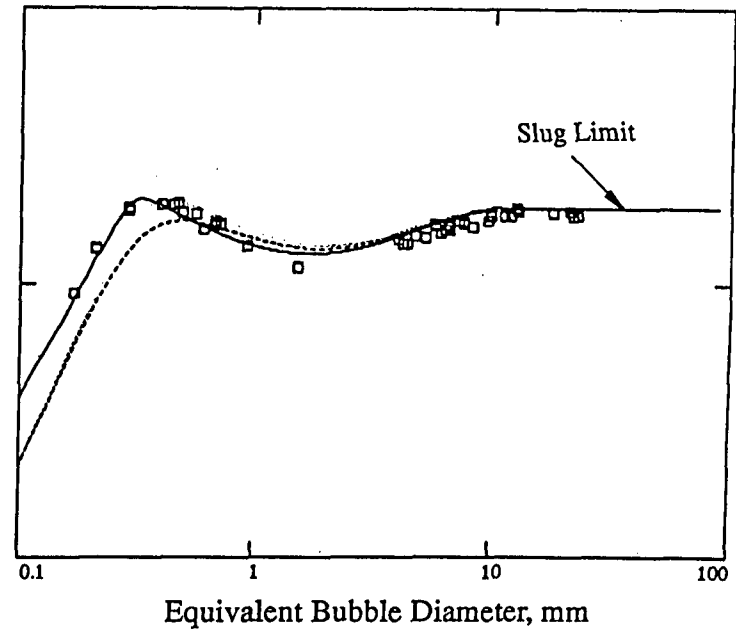
Figure 9

Comparison of Predicted Rise Velocity with Experimental SUVA Results

— Present Model: $C=1.0, \eta=8.0$
- - - Fan-Tsuchiya Model: $C=1.2, \eta=1.6$



(a) Dispersed Phase: SUVA



(b) Dispersed Phase: Nitrogen

28

Figure 10
 Comparison of Predicted Rise Velocity with
 Experimental Turpentine Results [Haberman and Morton, 1953]

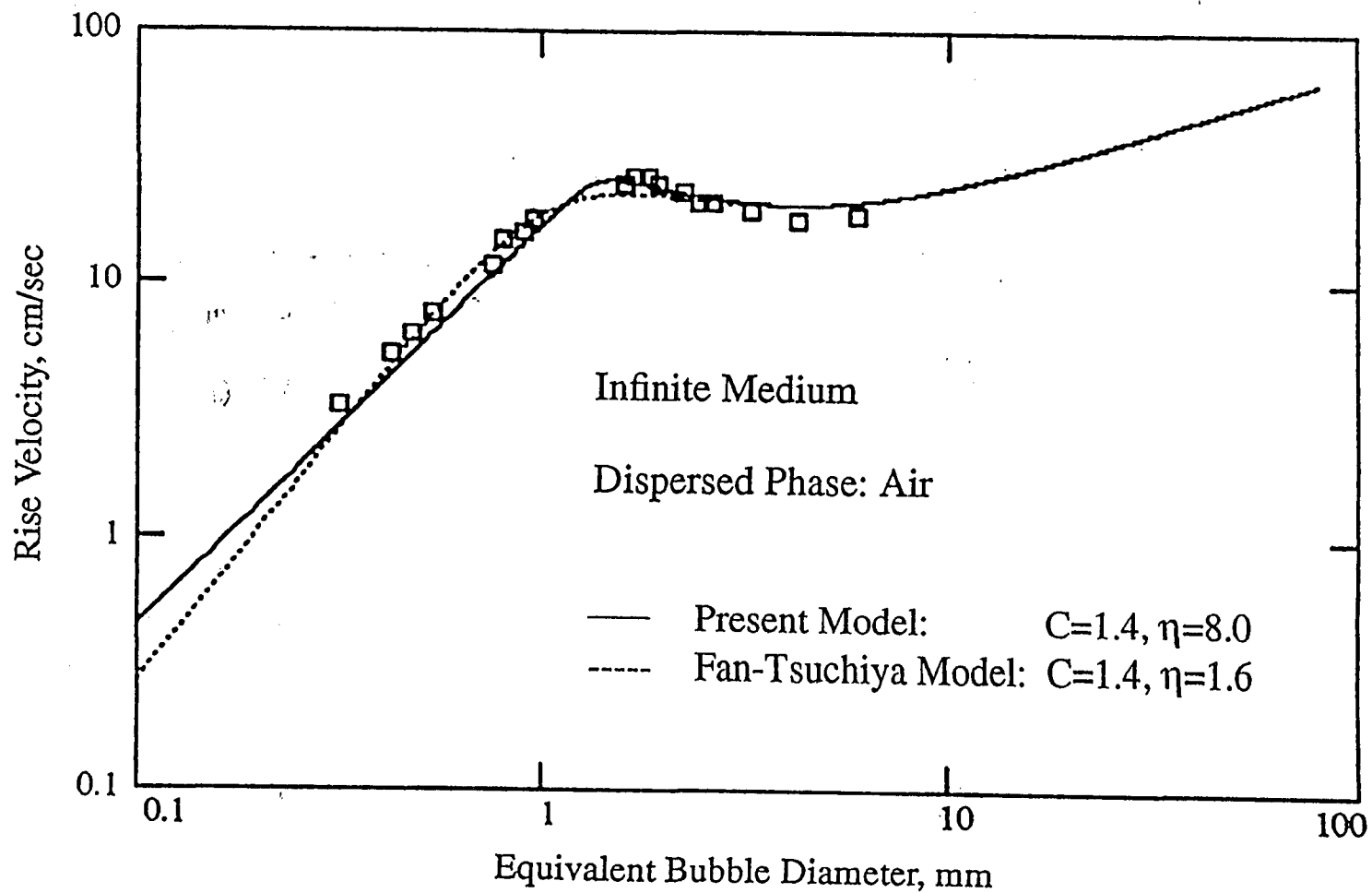


Figure 11
Comparison of Predicted Rise Velocity with
Experimental Varsol Results [Haberman and Morton, 1953]

